Novel layered structures constructed from metal(II)–chloranilate monomer compounds

Satoshi Kawata,[a]* Hitoshi Kumagai,[c] Keiichi Adachi[a] and Susumu Kitagawa[b]

[a] *Department of Chemistry, Shizuoka University, Shizuoka 422-8529, Japan.
E-mail: scskawa@ipc.shizuoka.ac.jp*
[b] *Graduate School of Engineering, Department of Synthetic Chemistry and
Biological Chemistry, Kyoto University, Yoshida, Sakyo-ku, Kyoto, 606-8501, Japan*
[c] *Institute for Molecular Science, Myoudaiji, Okazaki, Aichi 444-8585, Japan*

The new copper(II) and cobalt(II) assembled compounds $\{(G)_2[M(CA)_2(H_2O)_2]\}_n$ (M = Cu^{2+}, Co^{2+}; H_2CA = chloranilic acid; G = 4-hydroxypyridinium cation (4-pyOH_2^+), 3-hydroxypyridinium cation (3-pyOH_2^+)) have been synthesized and characterized. In every compound two chloranilate dianions and two water molecules are coordinated to the metal ion making dianionic monomers, $[M(CA)_2(H_2O)_2]^{2-}$. The coordination environment around the metal ion is a distorted octahedron, where two water molecules sit in a *trans* position to each other. $[M(CA)_2(H_2O)_2]^{2-}$ anions form anionic layer structures (**1**, **3**) and an anionic chain structure (**2**) by using hydrogen bonding interactions. The cations are introduced between the $\{[M(CA)_2(H_2O)_2]^{2-}\}_l$ layers or chains, which are supported by both the hydrogen bonding interaction and the electrostatic interaction between the organic cations and the complexes. In compounds **1** and **3**, the organic cations are stacked on each other to form a segregated columnar structure between the $\{[M(CA)_2(H_2O)_2]^{2-}\}_l$ layers. On the other hand, in compound **2**, the cations are included in a cage as a dimer. The cage is constructed by the chlorine atoms of CA^{2-} dianions of the chains and the organic cations are anchored to the chain by the hydrogen bonding interactions.

Introduction

Construction of assembled metal complexes with specific network topologies is an important step to realize not only a new magnetic and conductive phase,[1–13] but also an inclusion or intercalation system for ion- or molecule-exchange,[14,15] adsorption[16–21] and catalytic properties[22] due to their fascinating molecular structures.[23–41] Intermolecular interactions that have been used to produce such networks include coordination bonding,[42–44] hydrogen bonding,[45–54,85] and van der Waals forces such as stacking interactions.[55–59] Especially, the hydrogen bonding interaction is relevant to realize higher dimensional metal complex assemblies with novel properties such as microporosity,[44,60] dynamic properties concerning proton-transfer-mediated electron transfer through the hydrogen bond,[61–63] non-linear optics[64] and thermochromic properties of the crystal forms. Thus one of the best strategies for the rational synthesis of crystalline metal assemblies is to utilize the hydrogen bonding capability of coordinated ligands in addition to their coordination capability. On the other hand, compounds with layer or chain structure can intercalate (include) small molecules.[65–69] On the basis that hydrogen bonding is also the attractive force in cooperation with guest molecules, the organic molecules having multihydrogen bonding sites would be included into compounds having layer or chain structure.

Very recently, taking advantage of the strong hydrogen bonding ability of a pyridine hydroxyl group and an oxocarbon hydroxyl group, we prepared the novel intercalation compounds which consist of the straight 1-D chain, $[M(CA)\text{-}(H_2O)_2]_k$ (M = Mn^{2+}, Fe^{2+}, Co^{2+}, Cu^{2+}; H_2CA = chloranilic acid ($C_6H_2O_4Cl_2$)) and uncoordinated guest molecules.[70,71] The chains are linked by hydrogen bonds between the coordinated water and the oxygen atoms of the CA^{2-} anion on the adjacent chain, forming layers. The guest molecules are intercalated

between the $\{[M(CA)(H_2O)_2]_k\}_l$[86] layers, which are supported by N $\cdots$ H_2O hydrogen bonding. Although the layers are flexible, only neutral and symmetrical guest molecules are introduced between the layers. In spite of the importance of hydrogen bonding between cations and anions for supra-molecular assembly and molecular recognition in biological systems and functional materials, to date only a small number of organic and metal–organic supramolecular hydrogen bonded frameworks have been constructed using exclusively ionic compounds.[24,46,60,72,73] However, detailed control over the assembly and arrangement of ions in solid materials proves to be an illusory goal and further work is required in order to increase the choice of reliable building blocks and, more importantly, to allow us to rationalize and predict structural arrangements and functionalities of such materials.[74]

In considering the remarkable hydrogen bonding properties exhibited by the 1-D metal–chloranilate system, we are reminded of two-dimensional hydrogen bond-supported sheets, $\{[Fe(CA)_2(H_2O)_2]^-\}_l$ which intercalate ferrocenium cations and phenazinium cations.[75,76] The charged molecule is introduced between the $\{[Fe(CA)_2(H_2O)_2]^-\}_l$ layers, and is supported by the electrostatic interaction. The extension of this chemistry would afford new hydrogen bonding assemblies if the layered compounds are constructed using similar building blocks and include charged molecules with functionalities such as conducting and/or photosensitized properties by using hydrogen bonding interactions. In this study, we propose a new synthetic strategy to take advantage of the anionic complex, $[M(CA)_2\text{-}(H_2O)_2]^{m-}$ as a hydrogen bonding module for constructing various structures of assembled compounds. The monomer complex has two oxygen atoms at axial sites and eight oxygen atoms on the coordinated chloranilates in the equatorial plane, thus it is an attractive functional module to use in designing the lattice structure. The coordinated waters and terminal oxygen on the chloranilates operate as hydrogen bonding donors and

acceptor, respectively, to form two types of structural motif; one-dimensional (tape) and two-dimensional (sheet) illustrated as Scheme 1.[37,45,77] The "tape" motif has a remaining hydrogen
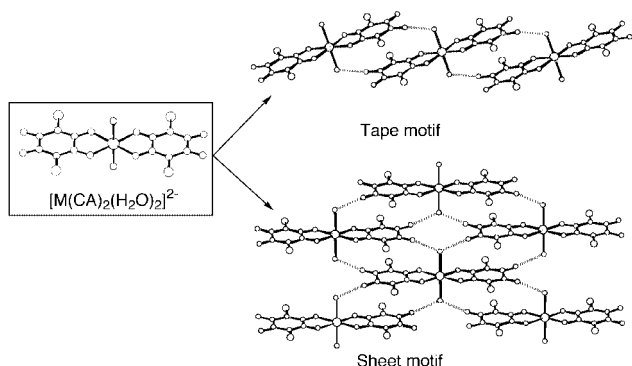
Scheme 1

bonding donor site on each coordinated water and hydrogen bonding acceptor sites on the chloranilates and waters while the "sheet" motif has only acceptor sites, suggesting that the interaction modes of the anionic motifs to the cations are different from each other.

To develop the supramolecular chemistry of the metal–chloranilate system, we describe here novel one- and two-dimensional hydrogen bond-supported compounds which are constructed from the monomer and charged organic cations, $\{(G)_m[M(CA)_2(H_2O)_2]\}_n$ ($M^{2+} = Cu^{2+}$, Co^{2+}; G = 4-hydroxypyridinium (4-pyOH$_2^+$), 3-hydroxypyridinium (3-pyOH$_2^+$); CA^{2-} = chloranilate ($C_6Cl_2O_4$)). The organic cations are introduced between the $\{[M(CA)_2(H_2O)_2]^{2-}\}_l$ chains or layers, which are supported by both the hydrogen bonding interaction and the electrostatic interaction between the cations and the anionic complexes. We discuss the factors that determine the structures of organic–inorganic molecular composites. In addition to the crystal structures, magnetic and thermal properties are also described.

Experimental

Synthesis of $\{(4\text{-pyOH}_2)_2[Cu(CA)_2(H_2O)_2]\}_n$ (1)

An aqueous solution (3 ml) of copper sulfate pentahydrate (1 mmol l^{-1}) was transferred to a glass tube, then an ethanol–water mixture (3 ml) of 4-pyOH (2 mmol l^{-1}) and H$_2$CA (2 mmol l^{-1}) was poured into the tube without mixing the two solutions. Red-purple plate crystals began to form at ambient temperature within a week. One of these crystals was used for X-ray crystallography. Anal. Calcd. for CuCl$_4$O$_{12}$C$_{22}$H$_{16}$N$_2$: C, 37.44; H, 2.29; N, 3.97%. Found: C, 37.41; H, 2.42; N, 3.93%.

Synthesis of $\{(3\text{-pyOH}_2)_2[Cu(CA)_2(H_2O)_2]\}_n$ (2)

Compound **2** was synthesized from copper sulfate and 3-pyOH, respectively, by a procedure similar to that employed for **1**. Red-purple plate crystals began to form within a week. One of these crystals was used for X-ray crystallography. Calcd. for CuCl$_4$O$_{12}$-C$_{22}$H$_{16}$N$_2$: C, 37.44; H, 2.29; N, 3.97%. Found: C, 37.35; H, 2.21; N, 3.91%.

Synthesis of $\{(3\text{-pyOH}_2)_2[Co(CA)_2(H_2O)_2]\}_n$ (3)

Compound **3** was synthesized from cobalt sulfate and 3-pyOH, respectively, by a procedure similar to that employed for **2**. Red-purple plate crystals began to form within a week. One of these crystals was used for X-ray crystallography. Calcd. for CoCl$_4$O$_{12}$C$_{22}$H$_{16}$N$_2$: C, 37.69; H, 2.30; N, 4.00%. Found: C, 37.48; H, 2.32; N, 3.94%.

Physical measurements

IR spectra of the KBr discs were measured on a Hitachi I-5040

FT-IR spectrophotometer. UV and visible spectra were measured on a Hitachi U-3500 spectrophotometer. EPR spectra were recorded at the X-band frequency with a JEOL RE-3X spectrometer operating at 9.1–9.5 GHz. Resonance frequency was measured on an Anritsu MF76A microwave frequency counter. Magnetic fields were calibrated by an Echo Electronics EFM-2000AX NMR field meter. The EPR spectra were measured with a modulation frequency of 100 kHz and a modulation amplitude of 0.5 mT, throughout. X-Ray powder diffraction data were collected on a MAC Science MXP18 automated diffractometer by using Cu-Kα radiation. Thermal gravimetric (TG) analysis and differential scanning calorimetry (DSC) were carried out with a Seiko Instruments SSC5200 thermo-analyzer in a nitrogen atmosphere (heating rates: 10 K min^{-1} for TG; 2–5 K min^{-1} for DSC).

Crystallographic data collection and structure refinement

A suitable crystal was chosen and mounted on a glass fiber with epoxy resin. Data collections for compounds **1** and **3** were carried out on a Rigaku AFC7R with graphite-monochromated Mo-Kα radiation. Data collections for compound **2** were carried out on a MAC Science MXC3 with graphite-monochromated Mo-Kα radiation. Crystallographic data are given in Table 1. The structures were solved by direct methods (Rigaku TEXSAN crystallographic software package of Molecular Structure Corporation). All the hydrogen atoms were located in the Fourier difference maps. However, they were not refined.

CCDC reference number 186/2010.

See http://www.rsc.org/suppdata/dt/b0/b001822h/ for crystallographic files in .cif format.

Results and discussion

Crystal structure of $\{(4\text{-pyOH}_2)_2[Cu(CA)_2(H_2O)_2]\}_n$ (1)

The structure of **1** consists of a mononuclear [Cu(CA)$_2$-(H$_2$O)$_2$]$^{2-}$ dianion and 4-pyOH$_2^+$ cation. An ORTEP[87] drawing of **1** is shown in Fig. 1a, and selected bond distances and angles with their estimated standard deviations are listed in Table 2. The geometry around the metal ion of the monomer is a distorted octahedron involving the four oxygen atoms of two CA^{2-} anions and two water molecules which are *trans* to each other. The environment of the copper atom consists of the four short in-plane bonds and the two long axial bonds (1.962(2) Å (Cu–O(1) and Cu–O(1′)), 1.937(2) Å (Cu–O(2), Cu–O(2′)) and 2.623(3) Å (Cu–O(5), Cu–O(5′))), giving rise to a "4 + 2" type of configuration, and the copper atom sits on the equatorial plane. The axial bond distances are much longer than the equatorial ones and are comparable with those of [Cu$_2$(oxalate)$_2$(pyrazine)$_3$]$_n$ (Cu–N distance: 2.670(8) Å), indicative of weak coordination. Interestingly, [Cu(CA)$_2$(H$_2$O)$_2$]$^{2-}$ dianions of **1** form a "tape" motif extended to the diagonal between the *a*- and *c*-axes (Fig. 1b). The tapes are supported by both the stacking interaction and the hydrogen bonding interaction: the adjacent [Cu(CA)$_2$(H$_2$O)$_2$]$^{2-}$ dianions are stacked on each other with coordinated chloranilate, the distance of the neighbor C(1)–C(3′) being 3.387(4) Å, to support the tape, and hydrogen bonds (O(3)–O(5″); 2.684(3) Å) occur between the coordinated water and the oxygen atom of CA^{2-} on the nearest neighbor complex. Moreover, the tape motifs, are fabricated into a layer, $\{[Cu(CA)_2(H_2O)_2]^{2-}\}_l$ spreading out along the *ac*-plane (Fig. 1b). This "sheet" motif is supported by hydrogen bonds (O(4)–O(5″); 2.765(3) Å), which occur between the coordinated water and the oxygen atom of CA^{2-} on the adjacent complex in the tape. The chlorine atoms of CA^{2-} project forward to the outside of the layer to create channels along the *c*-direction. The 4-pyOH$_2^+$ cations are included in the channel (Fig. 1c). This feature resembles the structures of $\{[Fe(Cp)_2][Fe(CA)_2(H_2O)_2]\}_n$ and $\{(Hphz)[Fe(CA)_2(H_2O)_2]$-
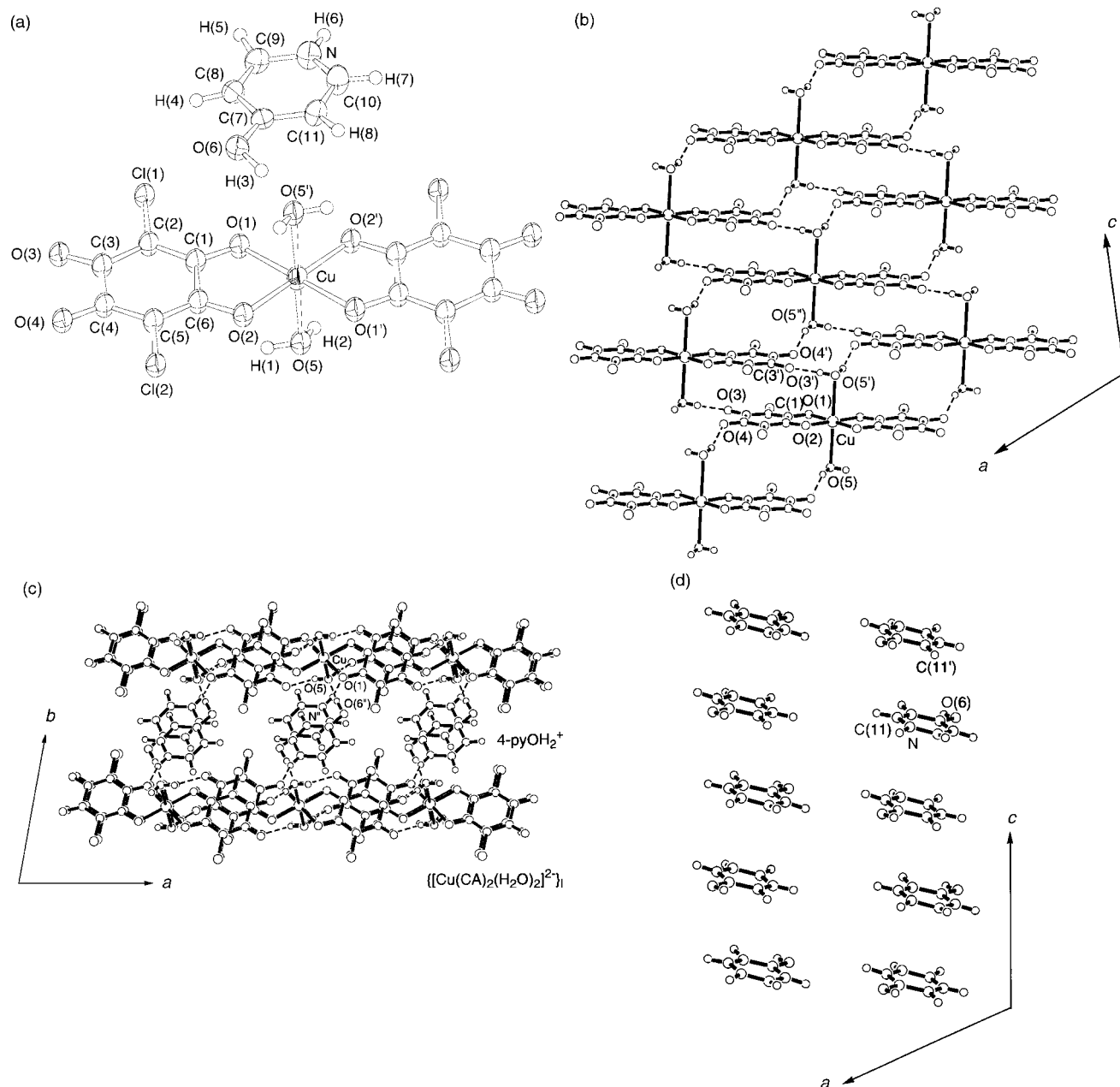
Fig. 1 (a) ORTEP drawing of a monomer unit of compound **1** with labeling scheme and thermal ellipsoids at the 50% probability level for Cu, Cl, O, and C atoms. Spheres of the hydrogen atoms have been arbitrarily reduced. (b) Sheet structure of $\{[Cu(CA)_2(H_2O)_2]^{2-}\}_l$. (c) Projection of **1** along the c-axis. (d) Columnar structure of 4-pyOH$_2^+$ cations in **1**. The dashed lines denote the sites of hydrogen bonding between the ions.

$(H_2O)_2\}_n$ (phz = phenazine), suggesting that the electrostatic interaction between the complex and the cation plays an important role to introduce the organic cation between the layer. Moreover, two kinds of hydrogen bonding occur between the uncoordinated 4-pyOH$_2$ and the coordinated water on the complex (O(5)–O(6″); 2.593(3) Å, N″–O(1); 3.049(4) Å). These bonds interlink the nearest-neighbor sheets to afford a three-dimensional structure and rivet the conformation/orientation of the cations, in other words, provide a novel assemblage stabilized by both hydrogen bonding interactions and electrostatic interactions between the ions. On the other hand, organic cations, 4-pyOH$_2^+$ are stacked on each other along the c-axis (nearest neighbor C(11)–C(11′) distance: 3.418(7) Å) to form a columnar structure in the channel (Fig. 1d). Therefore, stacking modes of the organic cations are affected by the assembled structures of the anionic complexes (*vide infra*).

### Crystal structure of $\{(3\text{-pyOH}_2)_2[Cu(CA)_2(H_2O)_2]\}_n$ (2)

The structure of **2** consists of a mononuclear [Cu(CA)$_2$-$(H_2O)_2]^{2-}$ dianion and a 3-pyOH$_2^+$ cation. An ORTEP drawing of **2** is shown in Fig. 2a, and selected bond distances and angles with their estimated standard deviations are listed in Table 2. The symmetry around the copper ion of the monomer is similar to that of **1** and slightly higher than that of **1** (1.946(3) Å (Cu–O(1), Cu–O(1′)), 1.944(3) Å (Cu–O(2), Cu–O(2′)) and 2.499(4) Å (Cu–O(3), Cu–O(3′))). However, crystal packing structure of **2** is different from that of **1**, that is, the [Cu(CA)$_2$(H$_2$O)$_2]^{2-}$ dianions of **2** do not form layers but tapes, $\{[M(CA)_2(H_2O)_2]^{2-}\}_k$. The "tape" motif extends to the b-axis and is supported by hydrogen bonds (O(3)–O(4″); 2.771(5) Å), which occur between the coordinated water and the oxygen atom of CA^{2-} on the nearest neighbor complex (Fig. 2b). Moreover, the adjacent [Cu(CA)$_2$(H$_2$O)$_2]^{2-}$ dianions are stacked on each other with coordinated chloranilate, the distance of the neighbor C(2)–C(4″) being 3.313(7) Å, to support the tape. These features resemble those of **1** very closely. Interestingly, four tapes surround the included 3-pyOH$_2^+$ cations. Each cation has the same geometry as do the cations in related compounds.[43,78–81] The twelve chlorine atoms of the CA^{2-}

Table 1 Crystallographic data for $\{(4\text{-pyOH}_2)_2[\text{Cu(CA)}_2(\text{H}_2\text{O})_2]\}_n$ (1), $\{(3\text{pyOH}_2)_2[\text{Cu(CA)}_2(\text{H}_2\text{O})_2]\}_n$ (2), and $\{(3\text{-pyOH}_2)_2[\text{Co(CA)}_2(\text{H}_2\text{O})_2]\}_n$ (3)

Compound	1	2	3
Formula	$\text{CuCl}_4\text{O}_{12}\text{C}_{22}\text{H}_{16}\text{N}_2$	$\text{CuCl}_4\text{O}_{12}\text{C}_{22}\text{H}_{16}\text{N}_2$	$\text{CoCl}_4\text{O}_{12}\text{C}_{22}\text{H}_{16}\text{N}_2$
FW	705.73	705.73	701.12
Dimensions/mm	$0.20 \times 0.10 \times 0.10$	$0.70 \times 0.40 \times 0.04$	$0.20 \times 0.05 \times 0.05$
Space group	$P\bar{1}$ (no. 2)	$P2_1/n$ (no. 14)	$P\bar{1}$ (no. 2)
Crystal system	Triclinic	Monoclinic	Triclinic
a/Å	9.028(2)	13.720(4)	9.784(3)
b/Å	9.797(2)	9.562(5)	17.088(6)
c/Å	8.764(2)	9.656(2)	7.499(2)
a/°	113.17(2)		94.83(2)
β/°	117.23(1)	90.533(2)	100.86(2)
γ/°	71.65(2)		95.77(2)
V/Å³	625.0(2)	1266.9(6)	1218.2
Z	1	2	2
μ(Mo-Kα)/cm^{-1}	1.373	1.354	1.217
Diffractometer	AFC7R	MXC3X	AFC7R
T/°C	23.0	23.0	23.0
Unique reflections	2873	3087	5609
No. of observed reflections	1966	1912	3762
R^a	0.035	0.052	0.082
$R_w^{\,b}$	0.033	0.053	0.044
R(int)	0.031	0.052	0.070

^{a} $R = \Sigma||F_o| - |F_c||/\Sigma|F_o|$. ^{b} $R_w = [(\Sigma w(|F_o| - |F_c|)^2/\Sigma wF_o^2)]^{1/2}$, $w = [\sigma^2(F_o^2) + p^2/4*F_o^2]^{-1}$.
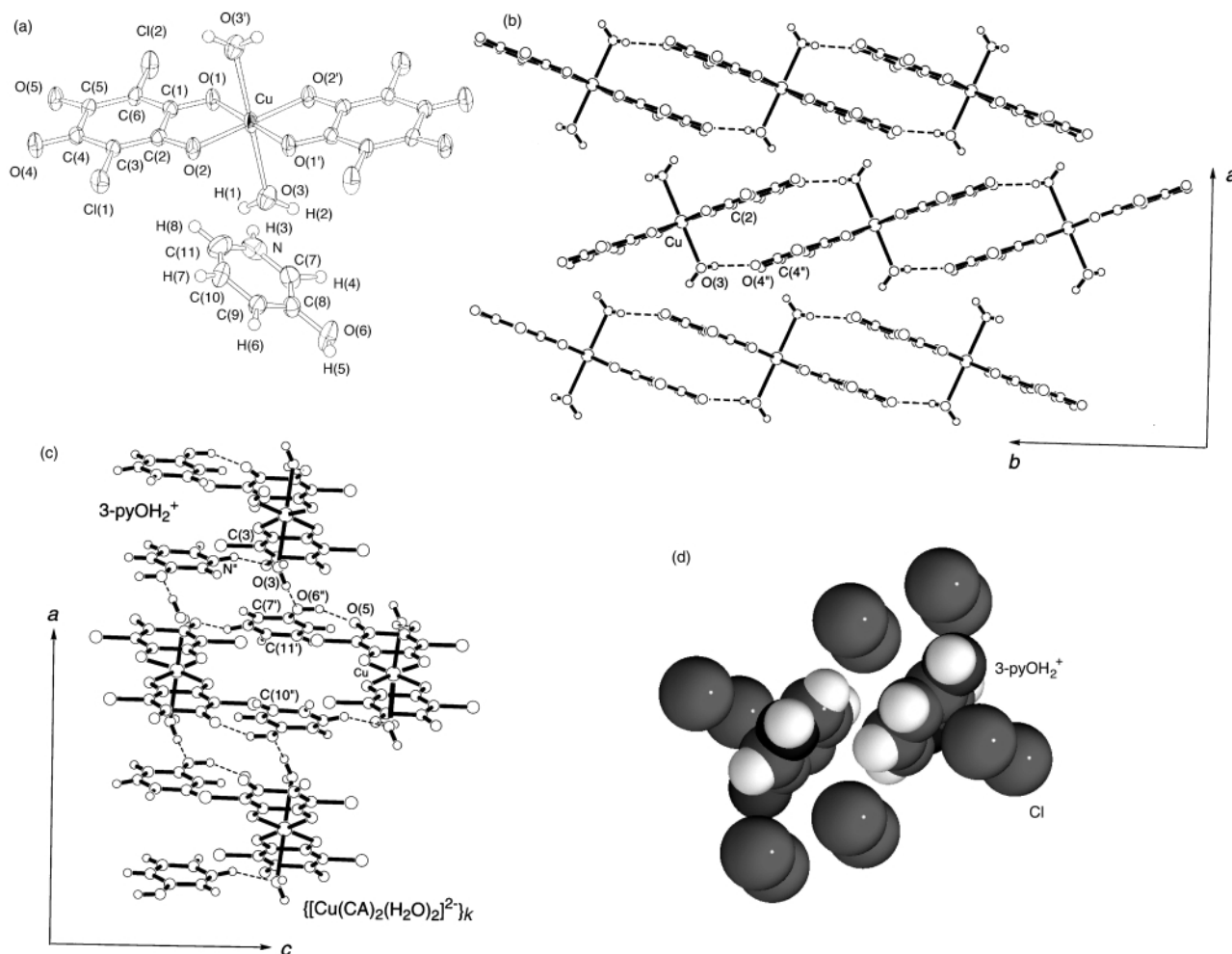
Fig. 2 (a) ORTEP drawing of a monomer unit of compound **2** with labeling scheme and thermal ellipsoids at the 50% probability level for Cu, Cl, O, and C atoms. Spheres of the hydrogen atoms have been arbitrarily reduced. (b) Tape structure of $\{[\text{Cu(CA)}_2(\text{H}_2\text{O})_2]^{2-}\}_k$. (c) Projection of **2** along the b-axis. The dashed lines denote the sites of hydrogen bonding between the ions. (d) Cage structure in **2**.

dianions of the adjacent tapes project out as thorns to create a cage, that is, eight Cl atoms on the monomer in two of the neighbor tapes and four Cl atoms on the chloranilates which stack with the cations (nearest neighbor C(3)–C(7′) distance: 3.366(8) Å) form a cage (Fig. 2c and 2d). Two 3-pyOH$_2^+$ cations

are included in the cage and stacked on each other to form a dimer (nearest neighbor C(11′)–C(10″) distance: 3.348(8) Å) and this interaction mode is different from that of **1**. Therefore it follows from a structural comparison between **1** and **2** that the packing mode of the cations depends on the arrangement of

Table 2 Bond distances (Å) and angles (°)

$\{(4\text{-pyOH}_2)_2[Cu(CA)_2(H_2O)_2]\}_n$ **(1)**

Cu–O(1)	1.962(2)	Cu–O(2)	1.937(2)
Cu–O(5)	2.623(3)	O(1)–C(1)	1.276(4)
O(2)–C(6)	1.274(4)	O(3)–C(3)	1.232(4)
O(4)–C(4)	1.234(4)	O(6)–C(7)	1.318(4)
O(1)–N″	3.049(4)	O(3)–O(5″)	2.684(3)
O(4)–O(5″)	2.765(3)	O(5)–O(6″)	2.593(3)

$\{(3\text{-pyOH}_2)_2[Cu(CA)_2(H_2O)_2]\}_n$ **(2)**

Cu–O(1)	1.946(3)	Cu–O(2)	1.944(3)
Cu–O(3)	2.499(4)	Cl(1)–C(3)	1.729(4)
O(2)–C(2)	1.275(5)	O(4)–C(4)	1.229(5)
O(5)–C(5)	1.244(5)	O(6)–C(8)	1.344(6)
O(3)–N	2.861(6)	O(3)–O(4″)	2.771(5)
O(3)–O(6″)	2.914(5)	O(5″)–O(6)	2.601(5)

$\{(3\text{-pyOH}_2)_2[Co(CA)_2(H_2O)_2]\}_n$ **(3)**

Co(1)–O(1)	2.077(4)	Co(1)–O(2)	2.069(4)
Co(1)–O(3)	2.125(4)	Co(2)–O(6)	2.076(4)
Co(2)–O(7)	2.065(4)	Co(2)–O(8)	2.114(4)
O(2)–C(2)	1.265(6)	O(3)–C(3)	1.278(6)
O(4)–C(5)	1.235(6)	O(5)–C(6)	1.250(6)
O(7)–C(8)	1.262(6)	O(8)–C(9)	1.281(6)
O(9)–C(11)	1.232(6)	O(10)–C(12)	1.249(6)
O(11)–C(14)	1.328(7)	O(12)–C(19)	1.331(7)
O(1)–O(9″)	2.756(6)	O(1)–O(10″)	2.786(6)
O(6)–O(4′)	2.704(6)	O(6)–O(5)	2.754(5)
O(11)–O(3′)	2.829(6)	O(12)–O(5′)	2.675(6)
N(1)–O(10′)	2.866(8)	N(2)–O(8′)	2.920(7)

$\{(4\text{-pyOH}_2)_2[Cu(CA)_2(H_2O)_2]\}_n$ **(1)**

O(1)–Cu–O(2)	83.79(9)	O(1)–Cu–O(2′)	96.21(9)
O(1)–Cu–O(5)	85.68(9)	O(1)–Cu–O(5′)	94.32(9)
O(2)–Cu–O(5)	94.35(9)	O(1)–Cu–O(5′)	85.65(9)
Cu–O(1)–C(1)	112.5(2)	Cu–O(2)–C(6)	113.4(2)

$\{(3\text{-pyOH}_2)_2[Cu(CA)_2(H_2O)_2]\}_n$ **(2)**

O(1)–Cu–O(2)	84.2(1)	O(1)–Cu–O(2′)	95.8(1)
O(1)–Cu–O(3)	94.2(1)	O(1)–Cu–O(3′)	85.8(1)
O(2)–Cu–O(3)	88.1(1)	O(2)–Cu–O(3′)	91.9(1)
Cu–O(1)–C(1)	112.4(3)	Cu–O(2)–C(2)	112.5(3)

$\{(3\text{-pyOH}_2)_2[Co(CA)_2(H_2O)_2]\}_n$ **(3)**

O(1)–Co(1)–O(2)	91.8(2)	O(1)–Co(1)–O(2′)	88.2(2)
O(1)–Co(1)–O(3)	87.9(2)	O(1)–Co(1)–O(3′)	92.1(2)
O(2)–Co(1)–O(3)	77.6(1)	O(2)–Co(1)–O(3′)	102.4(1)
O(6)–Co(2)–O(7)	92.5(2)	O(6)–Co(2)–O(7′)	87.5(2)
O(6)–Co(2)–O(8)	88.1(2)	O(6)–Co(2)–O(8′)	91.9(2)
O(7)–Co(2)–O(8)	78.0(1)	O(7)–Co(2)–O(8′)	102.0(1)
Co(1)–O(2)–C(2)	116.1(3)	Co(1)–O(3)–C(3)	112.9(3)
Co(2)–O(7)–C(8)	115.1(3)	Co(2)–O(8)–C(9)	113.5(3)

the chlorine atoms on the CA^{2-} dianions. On the other hand, three types of hydrogen bonding occur between the uncoordinated 3-pyOH$_2^+$ cation and the coordinated water. Two of them are in the cage (O(5)–O(6″); 2.601(5) Å, N″–O(3); 2.861(6) Å) and link the dimers and the chains to form a sheet spreading out along the *bc*-plane. Another hydrogen bond (O(3)–O(6″): 2.914(5) Å), where the coordinated water is a hydrogen bonding donor attached to the hydroxy group on 3-pyOH$_2^+$ cations, interlink the nearest-neighbor layers to afford a three-dimensional structure.

Crystal structure of $\{(3\text{-pyOH}_2)_2[Co(CA)_2(H_2O)_2]\}_n$ (3)

The assembled structure of **3** consists of a layer constructed from the $[Co(CA)_2(H_2O)_2]^{2-}$ dianions and 3-pyOH$_2^+$ cations which are introduced between the layers. An ORTEP drawing of the asymmetric unit and the symmetry-related fragments for **3** is shown in Fig. 3a, and selected bond distances and angles with their estimated standard deviations are listed in Table 2. There are two kinds of monomer unit in the layer. The geometries around the metal ions of the monomers are

similar to each other and distorted octahedrons involving the four oxygen atoms of two CA^{2-} anions and two water molecules which lie *trans* to one another. The environment of the cobalt atom also consists of the four short in-plane bonds and the two long axial bonds (2.077(4) Å (Co(1)–O(1) and Co(1)–O(1′)), 2.069(4) Å (Co(1)–O(2), Co(1)–O(2′)) and 2.125(4) Å (Co(1)–O(3), Co(1)–O(3′))) giving rise to a "4 + 2" type of configuration. However the equatorial plane of the complex is not parallel to the chloranilate plane and is dissimilar to those of **1** and **2**, that is, chloranilates coordinate to the cobalt atom asymmetrically. Such asymmetrical coordination of the CA^{2-} dianion is also reflected in the distances of the C–O bonds. This feature is different from that of $\{[Fe(Cp)_2]$-$[Fe(CA)_2(H_2O)_2]\}_n$ while the $[Co(CA)_2(H_2O)_2]^{2-}$ dianions in **3** also form layers, $\{[Co(CA)_2(H_2O)_2]^{2-}\}_l$ spreading out along the *bc*-plane. The sheets are supported by four different hydrogen bond (O(1)–O(9′); 2.756(6) Å, O(1)–O(10′); 2.786(6) Å, O(6)–O(4′); 2.704(6) Å, O(6)–O(5); 2.754(5) Å), which occur between the coordinated waters and the oxygen atoms of CA^{2-} on the adjacent complexes (Fig. 3b). Moreover, the $[Co(CA)_2(H_2O)_2]^{2-}$ dianions are stacked on each other with the coordinated chloranilate plane along the *c*-axis, the distance of the neighbor C(2)–C(11′) and C(6)–C(9″) being 3.602(8) and 3.646(8) Å, respectively, to support the layer. Therefore two kinds of building block are connected alternatively to form the sheet motif in **3** while only one kind of monomer building block is regularly distributed in the sheet motifs of $\{(Hphz)[Fe(CA)_2(H_2O)_2]$-$(H_2O)_2\}_n$ and $\{[Fe(Cp)_2][Fe(CA)_2(H_2O)_2]\}_n$. On the other hand, the tape motifs in **1** connect to form the sheet motif. These facts suggest that the shape and the bonding interaction of the introduced organic cation molecules may affect the inorganic assemblies.

The chlorine atoms of CA^{2-} project forward to the outside of the layer to create channels along the *c*-direction. Two kinds of 3-pyOH$_2^+$ cations are included in the channels (Fig. 3c) and provide the cross-link between adjacent layers of $[Co(CA)_2$-$(H_2O)_2]^{2-}$. This is achieved through two kinds of hydrogen bond occurring between each 3-pyOH$_2^+$ and the coordinated waters (O(11)–O(3′); 2.829(6) Å, N(1)–O(10′); 2.866(8) Å, O(12)–O(5′); 2.675(6) Å, N(2)–O(8′), 2.920(7) Å). Each 3-pyOH$_2^+$ cation has the same geometry as do the cations in compound **2** and the layered compound, 3-hydroxypyridinium hydrogen L-malate.[48] However, the assembled structures of the included cations are different from each other, that is, they are dimers in **2**, discrete cations in 3-hydroxypyridinium hydrogen L-malate and a column in **3**. The planar 3-pyOH$_2^+$ cations are stacked on each other along the *c*-axis (C(19)–C(20′), 3.321(8) Å, C(15)–C(14); 3.362(9) Å), and the stacking 3-pyOH$_2^+$ cations are lined up in the channel and form a segregated column. Therefore, stacking modes of the cations are affected by the inorganic assemblies. Especially, the structural difference between **2** and **3** may be due to the differences in coordination geometry between the cobalt ion and copper ion.

EPR spectral properties of 1 and 2

Despite the dramatic packing differences between **1** and **2**, both compounds display similar magnetic properties (Fig. 4). The EPR spectrum of the powder sample of **1** at 77 K has a signal with $g_\parallel = 2.308$ and $g_\perp = 2.068$, consistent with the elongated octahedral geometry, and a weak half-field transition band, indicative of the presence of magnetic exchange between the Cu^{2+} centers. The EPR spectrum of the powder sample of **2** at 77 K resembles that of **1** with $g_\parallel = 2.322$ and $g_\perp = 2.071$ and a weak half-field transition band. The smaller $g_\parallel$ values of **1** are attributed to the relatively larger crystal field strength in the coordination plane: the distance between the copper and the coordinated water of **1** is much longer than that of **2** indicating that the in-plane ligand field is stronger than that of **2**. Interestingly, while the spectral shapes show exchange narrowing
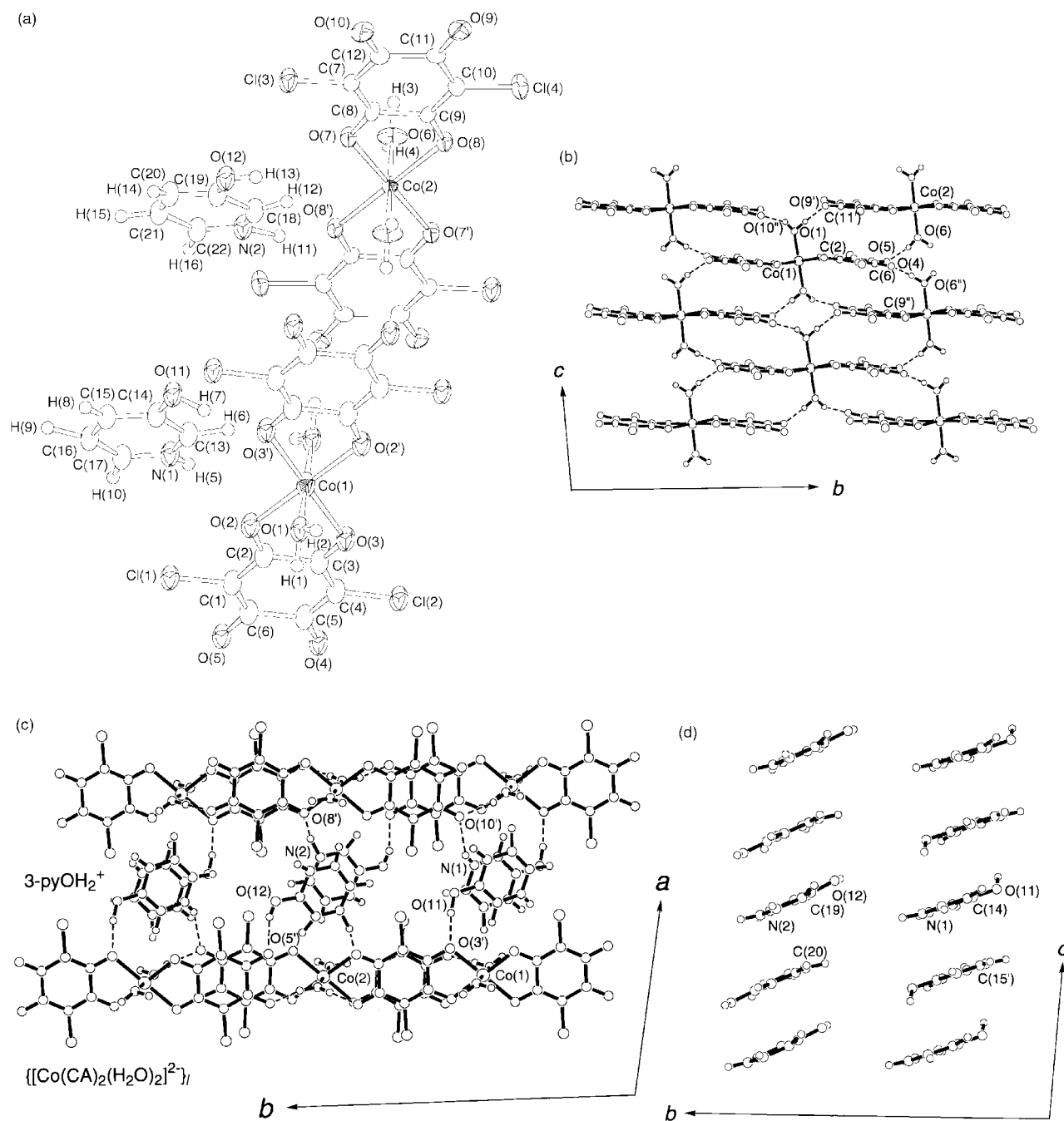
Fig. 3 (a) ORTEP drawing of a monomer unit of compound **3** with labeling scheme and thermal ellipsoids at the 50% probability level for Cu, Cl, O, and C atoms. Spheres of the hydrogen atoms have been arbitrarily reduced. (b) Sheet structure of $\{[Cu(CA)_2(H_2O)_2]^{2-}\}_l$. (c) Projection of **3** along the c-axis. (d) Columnar structure of 3-pyOH$_2^+$ cations in **3**. The dashed lines denote the sites of hydrogen bonding between the ions.

patterns in both complexes, the line widths in the $g_\perp$ region for **1** are broader than that for **2** indicative of the lower axial symmetry around the coordinated waters–copper axis of **1** than that of **2**, which is consistent with the X-ray structural results. On the other hand, line widths around the $g_\parallel$ region at $\Delta M_s = 1$ transition in both complexes are much broader than those in the $g_\perp$ region. These features are similar to that of a one-dimensional antiferromagnet, $[Cu(pyz)(NO_3)_2]_n$ (pyz = pyrazine) in which the direction of maximum line width in the EPR spectra is parallel to the principal axis of $g_\parallel$.[82–84] In compound **2**, the mononuclear Cu^{2+} building units are stacked on each other to make a "tape" motif and the angle between the tape direction and the principal axis of $g_\parallel$ which is normal to the chloranilate plane is about 30°. Thus a similar situation may hold for compound **2**. On the other hand, the maximum line width of a spectrum is normally found normal to the layer in the case of two dimensional compounds whereas it is not observed at such a direction which is parallel to the principal axis of $g_\perp$ in the case of **1**. These results suggest that the isotropic magnetic exchange interaction of **1** does not operate in the sheet motif but along the "tape" motif in which the running direction makes an angle of 35° with the principal axis of $g_\parallel$ normal to the chloranilate plane.

Thermal properties

The TG diagrams of **1** and **2** are given in Fig. 5. Weight losses of the compounds start at 105 °C and the liberation of water molecules accounts for the first weight loss (2H$_2$O, 5.1%) for both compounds. However, the liberation processes are different from each other: rapid and slow decreases are found in **1** and **2**, respectively. The species obtained upon liberation of the coordinated water molecules in the intermediate range 120–250 °C are assigned to $\{(G)_2[Cu(CA)_2]\}_n$ in both cases. These
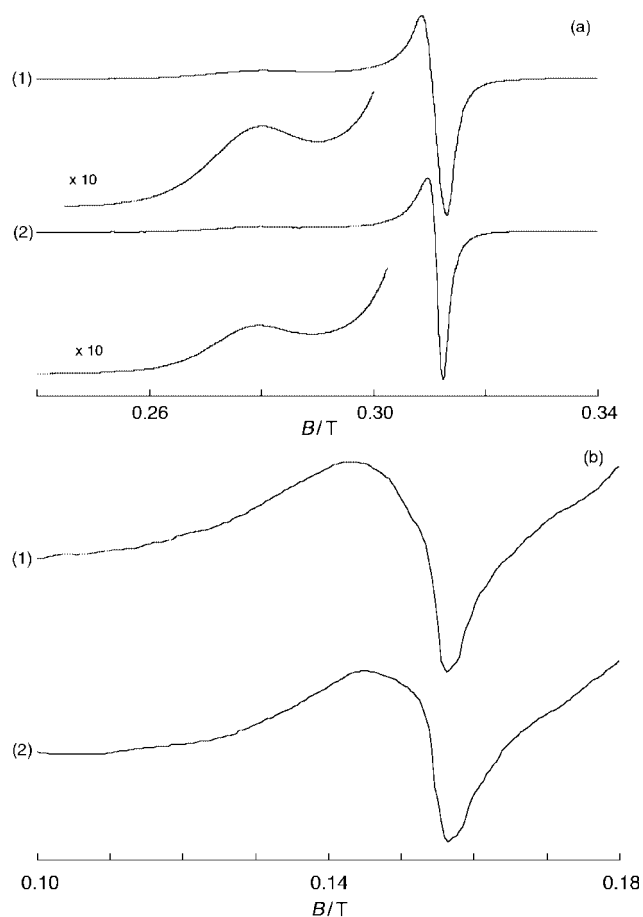
Fig. 4 Polycrystalline powder EPR spectra ((a), $\Delta M_s = 1$ region and (b) $\Delta M_s = 2$ region) of **1** (1) and **2** (2) at 77 K and $\nu = 9.0418$ GHz.

Fig. 5 Thermogravimetric analyses data for **1** (a) and **2** (b).

Fig. 6 Comparison of the X-ray powder diffraction patterns of **1** at 110 K (a) and 295 K (b). (c) shows the simulated pattern obtained from the crystal structure of **1**.

processes show that the coordinated water molecules are released easily compared with the interstitial organic molecules, indicative of the presence of large reconformation in the crystals. Especially, the included 4-pyOH$_2^+$ cation can change the orientation more easily than the 3-pyOH$_2^+$ cation, which is confirmed by the difference in the number of hydrogen bonds in the introduced cations.

It is worthwhile to examine the crystal structure change or the structural phase transition of the complexes in a lower temperature region to investigate the interaction between the cations and the anions. DSC traces of **1** show no drastic thermal anomaly in the lower temperature region while the XRD pattern of **1** shows the diffraction occurring from the $1 - 1 - 2$ lattice plane which indicates the distance between the planes of 4-pyOH$_2^+$, and that chloranilates on the adjacent complexes move towards each other (higher 2θ angle) with decreasing temperature while the 010 diffraction which indicates the distance between the layers does not shift (Fig. 6). On the other hand, the temperature dependence of NIR spectra for **1** show that OH or NH stretching vibrations change with decreasing temperature (Fig. 7). These facts suggest that the stacking distance or stacking mode of the organic cations changes with temperature and the hydrogen bonding interaction plays an important role in determining the crystal structure.

Conclusion

In this study, we have synthesized a new series of metal assemblies which contain hydrogen bonded building blocks in the complex assemblies and π-type stacking interaction of the organic cations. The assemblies of complex modules obtained here, that is, the hydrogen bond-supported inorganic assemblies, $\{[M(CA)_2(H_2O)_2]_k\}_l$, are so flexible that they can
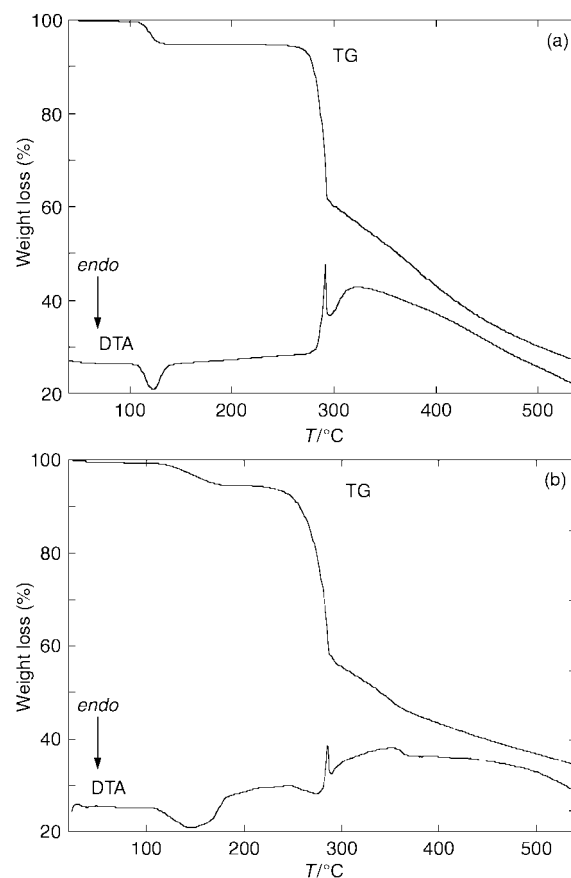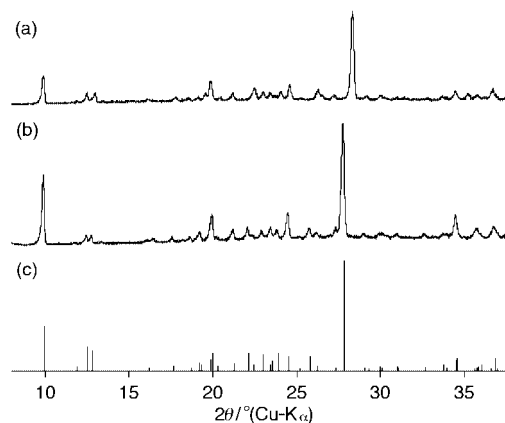
include various kinds of charged molecules by a change in the mode or dimension of the assembly: (1) channel-included type in **1** and **3**, and (2) cage-included type in **2**. For type 1 the organic cations are stacked to form a slipped stack column between the "sheet motifs", the layers of $\{[M(CA)_2(H_2O)_2]^{2-}\}_l$. The layer structure, which is modified by the hydrogen bonding and electrostatic interactions, influences the structure and the stacking mode of the included column. On the other hand, for type 2 the organic cations are trapped in the cage as a dimer. The cage is constructed by the chlorine atoms of CA^{2-} dianions of the tape motif and the cations are anchored by the hydrogen bonding interactions.

Both the electrostatic interaction and the hydrogen bonding interaction are driving forces to introduce the organic cations in these assemblies. In addition, the hydrogen bonding interaction
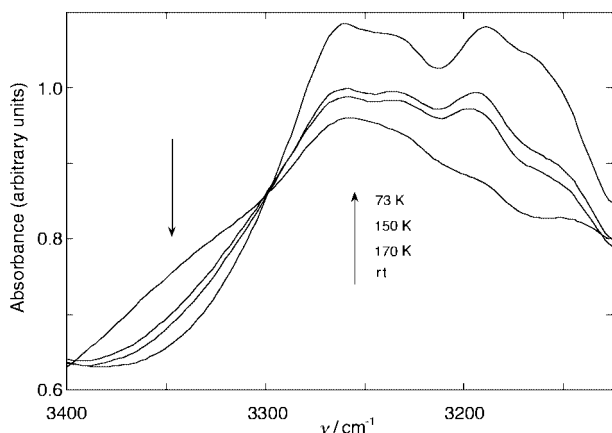
Fig. 7 Temperature dependence of the NIR spectrum of **1**.

increases the dimensionality of the system and thus provides structural varieties in the crystal structure. The crystallographic structures imply that in addition to having a hydrogen bonding support stacking capability an introduced molecule is important for the mode of assembly, and also show that selection of the metal mediates the tuning of the structure of the inorganic assemblies and the conformation of organic cations. The materials described here are composed of complex modules and organic cations. Further work will involve the ions which have potential functions such as conducting and/or photosensitized properties to further investigate this new synthesis strategy for functional materials.

Acknowledgements

References

1 D. W. Bruce and D. O'Hare, in *Inorganic Materials*, John Wiley & Sons, Chichester, 2nd edn., 1996.
2 O. Kahn, in *Magnetism: A Supramolecular Function*, Kluwer Academic Publishers, Dordrecht, 1996.
3 M. Kurmoo, A. W. Graham, P. Day, S. J. Coles, M. B. Hursthouse, J. L. Caulfield, J. Singleton, L. P. Francis, W. Hayes, L. Ducasse and P. Guionneau, *J. Am. Chem. Soc.*, 1995, **117**, 12209.
4 J. A. Real, E. Andrés, M. C. Muñoz, M. Julve, T. Granier, A. Bousseksou and F. Varret, *Science*, 1995, **268**, 265.
5 K. Inoue, T. Hayamizu, H. Iwamura, D. Hashizume and Y. Ohashi, *J. Am. Chem. Soc.*, 1996, **118**, 1903.
6 L. Ouahab, *Chem. Mater.*, 1997, **9**, 1909.
7 M. Umeya, S. Kawata, H. Matsuzaka, S. Kitagawa, H. Nishikawa, K. Kikuchi and I. Ikemoto, *J. Mater. Chem.*, 1998, **10**, 295.
8 H. Miyasaka, H. Okawa, A. Miyazaki and T. Enoki, *Inorg. Chem.*, 1998, **37**, 4878.
9 R. A. Heintz, H. Zhao, X. Ouyang, G. Grandinetti, J. Cowen and K. R. Dunber, *Inorg. Chem.*, 1999, **38**, 144.
10 O. Kahn and C. J. Martinez, *Science*, 1998, **279**, 44.
11 H. Kumagai and K. Inoue, *Angew. Chem., Int. Ed.*, 1999, **38**, 1601.
12 S. S. Turner, P. Day, K. M. A. Malik, M. B. Hurshouse, S. J. Teat, E. J. MacLean, L. Martin and S. A. French, *Inorg. Chem.*, 1999, **38**, 3543.
13 E. Coronado, J. Galán-Mascarós and C. J. Gómez-Garcia, *J. Chem. Soc., Dalton Trans.*, 2000, 205.
14 H. Li, A. Laine, M. O'Keeffe and O. M. Yaghi, *Science*, 1999, **283**, 1145.
15 H. Li, M. Eddaoudi, A. Laine, M. O'Keeffe and O. M. Yaghi, *J. Am. Chem. Soc.*, 1999, **121**, 6096.
16 O. M. Yaghi, G. Li and H. Li, *Nature*, 1995, **378**, 703.
17 L. Wang, P. Brazis, M. Rocci, C. R. Kannewurf and M. G. Kanatzidis, *Chem. Mater.*, 1998, **10**, 3298.
18 M. Kondo, T. Yoshitomi, K. Seki, H. Matsuzaka and S. Kitagawa, *Angew. Chem., Int. Ed. Engl.*, 1997, **36**, 1725.
19 M. Aoyaghi, K. Biradha and M. Fujita, *J. Am. Chem. Soc.*, 1999, **121**, 7457.
20 T. M. Reineke, M. Eddaoudi, M. Fehr, D. Kelley and O. M. Yaghi, *J. Am. Chem. Soc.*, 1999, **121**, 1651.
21 H. J. Choi, T. S. Lee and M. P. Suh, *Angew. Chem., Int. Ed.*, 1999, **38**, 1405.
22 M. Fujita, Y. J. Kwon, S. Washizu and K. Ogura, *J. Am. Chem. Soc.*, 1994, **116**, 1151.
23 S. Kitagawa and M. Kondo, *Bull. Chem. Soc. Jpn.*, 1998, **71**, 1739.
24 J.-M. Lehn, *Supramolecular Chemistry: Concepts and Perspectives*, VCH, Weinheim, 1995.
25 D. B. Amabilino and J. F. Stoddart, *Chem. Rev.*, 1995, **95**, 2725.
26 D. S. Lawrence, T. Jiang and M. Levett, *Chem. Rev.*, 1995, **95**, 2229.
27 G. M. Whitesides, *Sci. Am.*, 1995, 114.
28 C. Janiak, *Angew. Chem., Int. Ed. Engl.*, 1997, **36**, 1431.
29 M. Aoyagi, K. Biradha and M. Fujita, *J. Am. Chem. Soc.*, 1999, **121**, 7457.
30 S. Noro, M. Kondo, T. Ishii, S. Kitagawa and H. Matsuzaka, *J. Chem. Soc., Dalton Trans.*, 1999, 1569.
31 C. J. Kepert, D. Hesek, P. D. Beer and M. J. Rosseinsky, *Angew. Chem., Int. Ed.*, 1998, **37**, 3158.
32 S. Oliver, A. Kuperman and G. A. Ozin, *Angew. Chem., Int. Ed.*, 1998, **37**, 47.
33 H. J. Choi and M. P. Suh, *J. Am. Chem. Soc.*, 1998, **120**, 10622.
34 T. L. Breen, J. Tien, S. R. J. Oliver, T. Hadzic and G. M. Whitesides, *Science*, 1999, **284**, 948.
35 M. J. Plater, M. R. S. J. Foreman, E. Coronado, C. J. Gómez-García and A. M. Z. Slawin, *J. Chem. Soc., Dalton Trans.*, 1999, 4209.
36 H. Li, M. Eddaoudi and O. M. Yaghi, *Angew. Chem., Int. Ed.*, 1999, **38**, 653.
37 J. C. MacDonald and G. M. Whitesides, *Chem. Rev.*, 1994, **94**, 2383.
38 T. Kuroda-Sowa, T. Horino, M. Yamamoto, Y. Ohno, M. Maekawa and M. Munakata, *Inorg. Chem.*, 1997, **36**, 6382.
39 N. Masciocchi, G. A. Ardizzoia, G. LaMonica, A. Maspero and A. Sironi, *Angew. Chem., Int. Ed.*, 1998, **37**, 3366.
40 M. Fujita, N. Fujita, K. Ogura and K. Yamaguchi, *Nature*, 1999, **400**, 52.
41 P. V. Bernhardt, *Inorg. Chem.*, 1999, **38**, 3481.
42 M. Munakata, L. P. Wu, G. L. Ning, T. Kuroda-Sowa, M. Maekawa, Y. Suenaga and N. Maeno, *J. Am. Chem. Soc.*, 1999, **121**, 4968.
43 S. Kawata, S. R. Breeze, S. Wang, J. E. Greedan and N. P. Raju, *Chem. Commun.*, 1997, 717.
44 O. M. Yaghi, H. Li and T. L. Groy, *J. Am. Chem. Soc.*, 1996, **118**, 9096.
45 J. A. Zerkowski, C. T. Seto and G. M. Whitesides, *J. Am. Chem. Soc.*, 1992, **114**, 5473.
46 C. B. Aakeröy and K. R. Seddon, *Chem. Soc. Rev.*, 1993, 397.
47 J. P. Mathias, C. T. Seto, E. E. Simanek and G. M. Whitesides, *J. Am. Chem. Soc.*, 1994, **116**, 1725.
48 C. B. Aakeröy and M. Nieuwenhuyzen, *J. Am. Chem. Soc.*, 1994, **116**, 10983.
49 M. Munakata, L. P. Wu, M. Yamamoto, T. Kuroda-Sowa and M. Maekawa, *J. Am. Chem. Soc.*, 1996, **118**, 3117.
50 K. Endo, T. Ezuhara, M. Koyanagi, H. Masuda and Y. Aoyama, *J. Am. Chem. Soc.*, 1997, **119**, 499.
51 V. R. Pedireddi, S. Chatterjee, A. Ranganathan and C. N. R. Rao, *J. Am. Chem. Soc.*, 1997, **119**, 10867.
52 A. Ranganathan, V. R. Pedireddi and C. N. R. Rao, *J. Am. Chem. Soc.*, 1999, **121**, 1752.
53 M.-L. Tong, H. K. Lee, X.-M. Chen, R.-B. Huang and T. C. W. Mak, *J. Chem. Soc., Dalton Trans.*, 1999, 3657.
54 M. Tadokoro, K. Isobe, H. Uekusa, Y. Ohashi, J. Toyoda, K. Tashiro and K. Nakasuji, *Angew. Chem., Int. Ed.*, 1999, **38**, 95.
55 J. Dai, M. Yamamoto, T. Kuroda-Sowa, M. Maekawa, Y. Suenaga and M. Munakata, *Inorg. Chem.*, 1997, **36**, 2688.
56 P. V. Bernhardt and E. J. Hayes, *Inorg. Chem.*, 1998, **37**, 4214.
57 I. Unamuno, J. M. Gutiérrez-Zorrialla, A. Luque, P. Román, L. Lezama, R. Calvo and T. Rojo, *Inorg. Chem.*, 1998, **37**, 6452.
58 W. Lin, O. R. Evans, R.-G. Xiong and Z. Wang, *J. Am. Chem. Soc.*, 1998, **120**, 13272.
59 V. R. Thalladi, R. Boese, S. Brasselet, I. Ledoux, J. Zyss, R. K. R. Jetti and G. R. Desiraju, *Chem. Commun.*, 1999, 1639.
60 J. D. Martin and B. R. Leafblad, *Angew. Chem., Int. Ed.*, 1998, **37**, 3318.
61 K. Nakasuji, K. Sugiura, T. Kitagawa, J. Toyoda, H. Okamoto, K. Okinawa, T. Mitani, H. Yamamoto, I. Murata, A. Kawamoto and J. Tanaka, *J. Am. Chem. Soc.*, 1991, **113**, 1862.
62 C. F. Guerra and F. M. Bickelhaupt, *Angew. Chem., Int. Ed.*, 1999, **38**, 2942.
63 G. A. Jeffrey, *An Introduction of Hydrogen Bonding*, Oxford University Press, London, 1997.

64 C. C. Evans, M. Bagieu-Beucher, R. Masse and J.-F. Nicoud, *Chem. Mater.*, 1998, **10**, 847.

65 G. A. Ozin, *Adv. Mater.*, 1992, **4**, 612.

66 D. O'Hare, *New. J. Chem.*, 1994, **18**, 989.

67 J.-F. Nicoud, *Science*, 1994, **263**, 638.

68 A. Müller, H. Reuter and S. Dillinger, *Angew. Chem.*, *Int. Ed. Engl.*, 1995, **34**, 2328.

69 W. Fujita, K. Awaga and T. Yokoyama, *Inorg. Chem.*, 1997, **36**, 196.

70 S. Kawata, S. Kitagawa, H. Kumagai, C. Kudo, H. Kamesaki, T. Ishiyama, R. Suzuki, M. Kondo and M. Katada, *Inorg. Chem.*, 1996, **35**, 4449.

71 S. Kawata, S. Kitagawa, H. Kumagai, T. Ishiyama, K. Honda, H. Tobita, K. Adachi and M. Katada, *Chem. Mater.*, 1998, **10**, 3902.

72 M. C. T. Fyfe, P. T. Glink, S. Menzer, J. F. Stoddart, A. J. P. White and D. J. Williams, *Angew. Chem.*, *Int. Ed. Engl.*, 1997, **36**, 2068.

73 V. A. Russell, C. C. Evans, W. Li and M. D. Ward, *Science*, 1997, **276**, 575.

74 M. Scudder and I. Dance, *J. Chem. Soc.*, *Dalton Trans.*, 1998, 329.

75 S. Kawata, H. Kumagai, S. Kitagawa, K. Honda, M. Enomoto and M. Katada, *Mol. Cryst. Liq. Cryst.*, 1996, **286**, 51.

76 M. K. Kabir, S. Kawata, K. Adachi, H. Tobita, N. Miyazaki, H. Kumagai, M. Katada and S. Kitagawa, *Mol. Cryst. Liq. Cryst.*, 2000, in press.

77 J. A. Zerkowski, C. T. Seto, D. A. Wierda and G. M. Whitesides, *J. Am. Chem. Soc.*, 1990, **112**, 9025.

78 K. A. Byriel, C. H. L. Kennard, D. E. Lynch, G. Smith and J. Thompson, *Aust. J. Chem.*, 1992, **45**, 969.

79 U. Ohms, H. Guth and W. Treutmann, *Z. Kristallogr.*, 1983, **162**, 299.

80 D. E. Lynch and G. Smith, *Acta Crystallogr.*, *Sect. C*, 1992, **48**, 533.

81 Y. Ohgo and Y. Ohhashi, *Bull. Chem. Soc. Jpn.*, 1996, **69**, 2425.

82 K. T. Mcgregor and Z. Soos, *J. Chem. Phys.*, 1976, **64**, 2506.

83 D. Gatteschi and R. Sessoli, *Magn. Reson. Rev.*, 1990, **15**, 1.

84 A. Bencini and D. Gatteschi, *EPR of Exchange Coupled Systems*, Springer-Verlag, Berlin, 1990.

85 A. D. Burrows C.-W. Chan, M. M. Chowdhry, J. E. McGrady and D. M. P. Mingos, *Chem. Soc. Rev.*, 1995, 329.

86 k and l denote a one-dimensional and a two-dimensional assembly, respectively.

87 C. K. Johnson, ORTEP, Report ORNL-5138, Oak Ridge National Laboratory, Oak Ridge, TN, 1976.